Oceanic Engineering International, Vol. 2, No. 2, 1998, pp 54-64

Effect of Double-Peaked Wave Spectra on the Behaviour of Moored Semi-Submersibles

Oguz Yilmaz[1] and Atilla Incecik[2]

[1]*Istanbul Technical University, Faculty of Naval Architecture and Ocean Engineering, Maslak, Istanbul, 80626, Turkey.*
[2]*University of Newcastle upon Tyne, Department of Marine Technology, Armstrong Building, Newcastle upon Tyne, NE1 7RU, UK.*

email: atilla.incecik@newcastle.ac.uk

ABSTRACT

In this paper a non-linear time domain analysis procedure developed to predict the motion response of moored semi-submersibles under wave, wind, and current loading is described. Using the time domain model, behaviour of the semi-submersible in storm conditions is investigated. The wave spectrum considered in the study is a double-peaked JONSWAP spectrum. It is assumed that the ratio between the peaks and the peaked frequencies in a double-peaked spectrum depends on the location of the structure whether it is in the open ocean or in coastal waters. In both cases the behaviour of the semi-submersible is simulated using the time domain model

1. INTRODUCTION

Extreme weather conditions can cause mooring line failures or structural damage to semi-submersibles. Semi-submersible motions in a storm can be predicted using a time domain model which is capable of handling the non-linearities that exist in the system. Non-linearities could be due to the mooring lines, drag forces, damping, and large amplitude motions of the semi-submersible.

A Morison's equation based analysis was employed to calculate the wave forces acting on the semi-submersible, since the *D/l* ratios for semi-submersible members are less than 0.2 and the Keulegan Carpenter number is smaller than 5 even for very small frequencies. Extensive use of the theses by Incecik [1982] and Söylemez [1990] were made to formulate the wave forces. The effect of current was included in the drag force formulation by adding the current velocity to wave velocity. In calculating the wind forces, wind gustiness was taken into consideration using the Ochi-Shin spectrum [Ochi and Shin 1988]. Catenary equations were utilised to calculate the mooring forces. Details of the time domain model can be found in Yilmaz and Incecik [1995].

2. SEMI-SUBMERSIBLE USED IN THE STUDY

The semi-submersible used in the ITTC '93 comparative study [Pinkster *et al.* 1993] was chosen for the parametric study. The main characteristics of this semi-submersible are as follows:

- Pontoon dimensions; length: 115 m, breadth: 15 m, height: 9m;
- Column diameter: 11 and 9.5 m, Number of bracing members: 16;
- Column spacing; longitudinal: 25m, transverse: 60 m, draught: 24m;
- Displacement: 40796 m^3.

Mooring configuration of the semi-submersible is shown in figure 1. The semi-submersible has eight mooring lines and each one has a weight of 1.296 ton/m, initial tension of 200 kN, and length of 600 m. Water depth is 150 m.

The superstructure of the semi-submersible is given in figure 2. Projected areas and height and shape coefficients used for the wind force calculations are given below.

- Height coefficients: columns: 1
  deck house: 1.1
  hull: 1
  rig derrick: 1.37
  crane: 1.3
- Shape coefficients: columns: 0.5
  deck house: 1
  hull: 1
  rig derrick: 1.3
  crane: 1.5
- Columns projected area to wind = 820 m^2

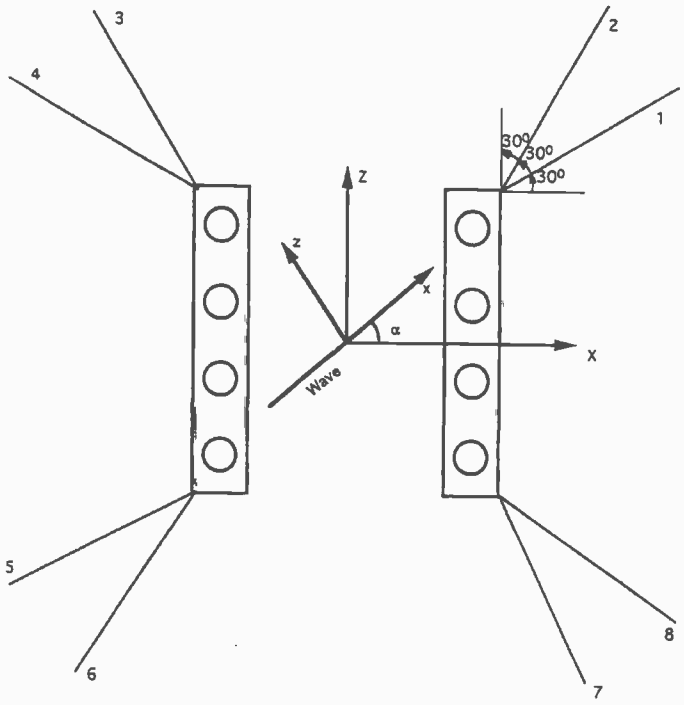

Figure 1 Mooring configuration and reference systems.

- Deck house projected area to wind in surge direction = 571 m^2.
- Deck house projected area to wind in sway direction = 664 m^2.
- Hull projected area to wind in surge direction = 480 m^2
- Hull projected area to wind in sway direction = 736 m^2.
- Rig derrick projected area to wind in surge direction = 449 m^2.
- Rig derrick projected area to wind in sway direction = 1011 m^2.
- Natural frequencies of the semi-submersible are as follows: 0.036 rad/sec for surge mode, 0.0307 rad/sec for sway mode, 0.255 rad/sec for heave mode and 0.0268 rad/sec for yaw mode.

3. TIME DOMAIN MODEL FOR A CATENARY MOORED SEMI-SUBMERSIBLE EXCITED BY WAVE, WIND AND CURRENT LOADING

Non-linear stiffness characteristics of the catenary mooring lines were taken into account in formulating the motion equations of the coupled system. The non-linear coupled motion equations were solved simultaneously in the time domain using a numerical integration technique. The technique adopted was the Adam's variable order variable step differential solver algorithm. In the time domain solutions of the motion equations, variable coefficients on the left hand side of these equations as well as the forcing functions on the right hand side of the equations were re-calculated thus taking into account the displaced position of the semi-submersible.

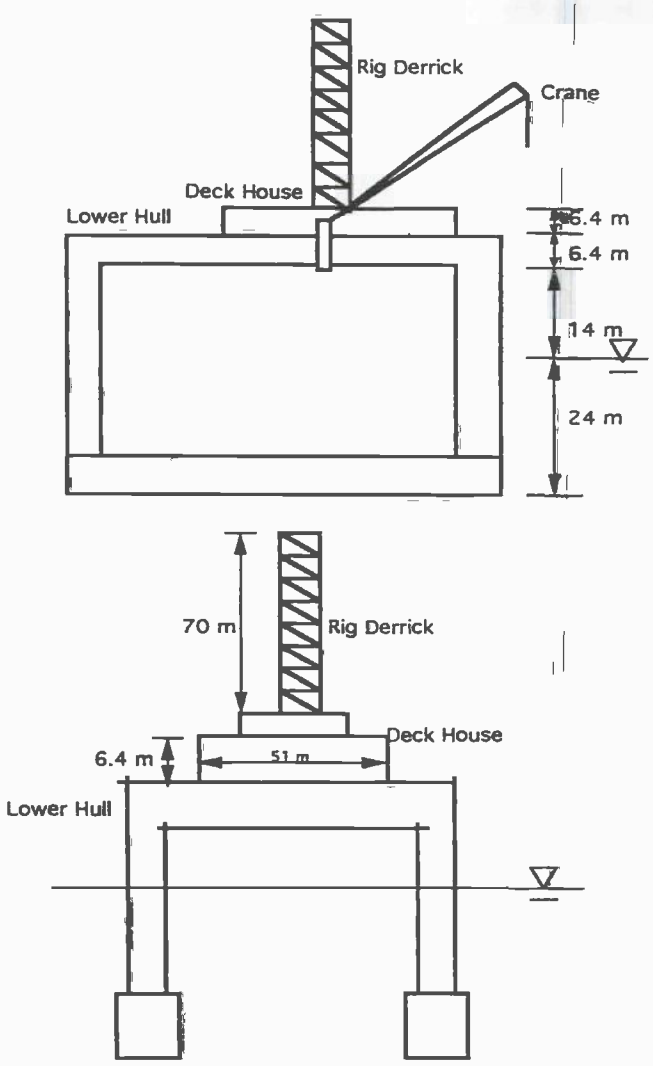

Figure 2. Semi-submersible superstructure.

In the moored semi-submersible system we considered only the surge, sway, heave, and yaw motions of the semi-submersible (see figure 1). Hence, the four degrees of freedom system can be written as follows:

$$M(\ddot{x} - z\dot{\theta}) + M_{AVM_x}\ddot{x} + b_x\dot{x}|\dot{x}| = F_{Ex} - F_{Mx}$$

$$M(\ddot{z} + x\dot{\theta}) + M_{AVM_z}\ddot{z} + b_z\dot{z}|\dot{z}| = F_{Ez} - F_{Mz}$$

$$(M + M_{AVM_y})\ddot{y} + b_y\dot{y}|\dot{y}| + k_y y = F_{Ey} - F_{My}$$

$$(I + I_{AVM_\theta})\ddot{\theta} + b_\theta\dot{\theta}|\dot{\theta}| = M_{E\theta} - M_{M\theta} \qquad (1)$$

where

x, z, y and θ indicate surge, sway, heave, and yaw modes respectively;
M is the mass of the semi-submersible;
I is the moment of inertia of mass of the semi-submersible in the yaw direction;

$M_{AVM,x}$ and $M_{AVM,z}$ are the added mass of the semi-submersible in the surge and sway directions respectively;
$I_{AVM,\theta}$ is the moment of inertia of added mass of the semi-submersible in the yaw direction;
b_x, b_z, b_y and b_θ are viscous damping coefficients;
k_y is the restoring coefficient in the heave direction;
F_{Ex}, F_{Ez}, F_{Ey} and $M_{E\theta}$ are wave, wind, and current forces and moments acting on the semi-submersible in surge, sway, heave, and yaw directions respectively;
F_{Mx}, F_{Mz}, F_{My} and $M_{M\theta}$ are the mooring forces and moment.

(a) Calculation of wave forces on semi-submersibles

It is assumed that Morison's equation is valid for cylinders of arbitrary orientation in deep and shallow water although it was originally developed for vertical cylinders. C_M and C_D coefficients for columns of the semi-submersible depicted in figure 1 are taken as 2 and 0.6 in surge and sway modes; for rectangular pontoons, 1.082 and 1.0 in surge mode; 1.76 and 1.0 in sway mode; and 3.09 and 1.0 in heave mode. C_M coefficients for pontoons are calculated using a 3-D program developed by Chan [1990]. In order to calculate the heave forces on columns Froude/Krylov and acceleration forces are calculated separately and the added mass of the columns are taken to be $4/3\rho R^3$. The effect of current is included in the study by modifying the velocity of the drag term of Morison's equation. Details of this can be found in Söylemez [1996].

(b) Evaluation of wind forces

The calculation of wind forces on offshore structures is a very difficult task requiring the use of empirical formulae. The Reynolds number largely determines the wind flow and the wind forces are calculated using a Morison type equation. Only the drag term of Morison's equation is important here because of the relatively low density and high compressibility of the air. Vortex shedding may occur causing vibration that is transverse to the flow direction. Fluctuations of the wind velocity acting upon the superstructures may have a large effect on the response of the offshore structures. By writing $V(t) = \overline{V} + v(t)$, the mean and dynamic wind forces are obtained as follows,

$$F_w^M(t) = \frac{1}{2}\rho_a C_D A_p \overline{V}^2 \qquad (2)$$

$$F_w^D(t) = \rho_a C_D A_p \overline{V}\, v(t) \qquad (3)$$

where

ρ_a is the air density (= 0.0012 t/m^3);
C_D is the drag coefficient = $C_h C_s$;
C_h is the height coefficient and C_s is the shape coefficient given in ABS [1973];
A_p is the projected area;
$V(t)$ is the time dependent wind velocity.

The wind spectrum used in this study was suggested by Ochi and Shin [1988] and was based on wind speed measurements carried out at sea. It has the following formulation.

$$S(f_*) = \begin{cases} 583 f_* & \text{for} \quad 0 \le f_* \le 0.00 \\ \dfrac{420 f_*^{0.70}}{(1 + f_*^{0.35})^{11.5}} & \text{for} \quad 0.003 \le f_* \le 0.1 \\ \dfrac{838 f_*}{(1 + f_*^{0.35})^{11.5}} & \text{for} \quad f_* \ge 0.1 \end{cases} \qquad (4)$$

where

f^* is the dimensionless frequency $f_n = f_z / \overline{V}_z$;
$S(f^*)$ is the dimensionless spectral density;
f is frequency in Hz;
z is the height above sea level in metres;
$\overline{V}_z$ is the mean wind speed at height z in m/sec;
$S(f)$ is the spectral density function in m^2/sec.

Time dependent velocity is obtained by the sum of sines approach with a random phase distribution:

$$V(t) = \overline{V} + \sum_{n=0}^{\infty} \sqrt{2S(\omega_n)\nabla\omega}\, \cos(\omega_n t + \varepsilon_n) \qquad (5)$$

4. OCCURRENCE OF DOUBLE-PEAKED WAVE SPECTRA IN EXTREME WEATHER CONDITIONS

Most of the existing mathematical wave spectra are single-peaked and are representative of wind driven seas. Many measured spectra exhibit two peaks when swell and wind seas are simultaneously present or when a refreshing or a changing wind direction creates a developing wave system [Guedes-Soares 1984]. There are two types of double peaked spectra mentioned by Guedes-Soares [1984]. One type of spectrum dominated by the high frequency peak is called a wind-dominated spectrum. The low frequency part of this spectrum is generated by a swell system that travels a considerable distance losing much energy. The other type of spectrum dominated by the low frequency peak is called a swell-dominated spectrum, and is generated either by a refreshing wind or by a change in wind direction which creates a system of short period waves coexistent with the old wave system. A double peaked spectrum is modelled with two JONSWAP types of spectra. If the ratios of peak frequencies and of spectral peaks are known then a double peaked spectrum can be described. If we represent the sea spectrum S by the sum of a swell S_S and a wind sea S_W component we get

$$S(\omega) = S_S(\omega) + S_W(\omega) \qquad (6)$$

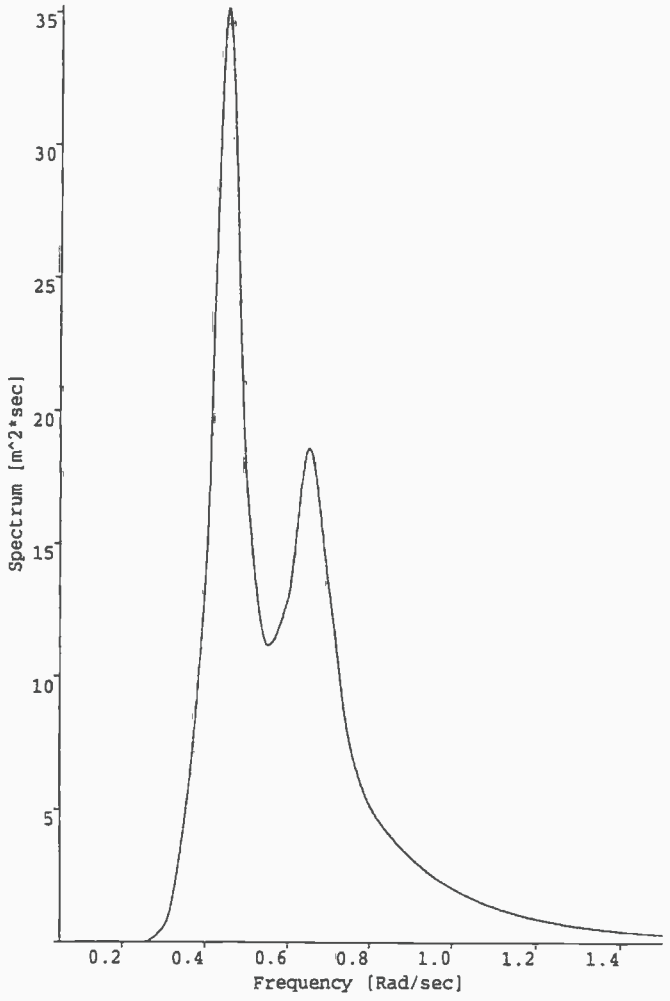

Figure 3. Double peaked wave spectrum for open ocean. Hs = 7m for wind waves, 9 m for swell waves. Tz = 7.5 sec for wind waves, 11 sec for swell waves.

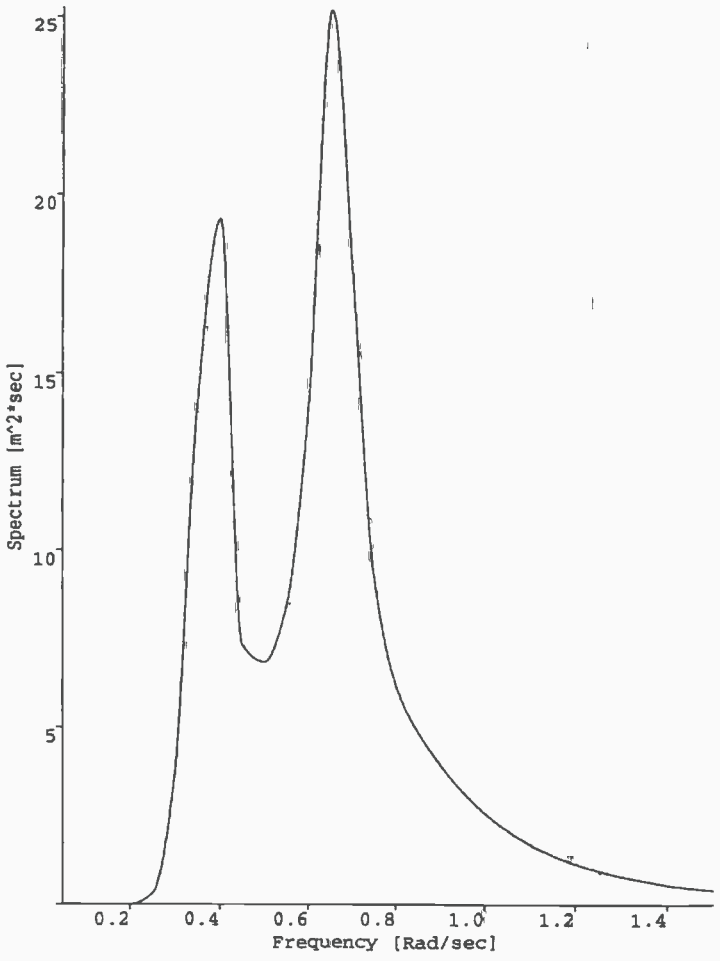

Figure 4. Double peaked wave spectrum for coastal waters. Hs = 9m for wind waves, 7 m for swell waves. Tz = 7.5 sec for wind waves, 11 sec for swell waves

A detailed formulation of a double peaked wave spectrum can be found in Guedes-Soares [1984]. It was concluded in the paper that the occurrence of double-peaked spectra decreases with increasing significant wave height, varying from 40% at lower sea states to 5% for high wave conditions and that double-peaked spectra occur less often in fetch limited coastal waters than in the open ocean. Another important conclusion was that swell dominated spectra occur more often in the open ocean than in coastal waters.

Relying on the investigations by Guedes-Soares, two different storm locations were considered: open ocean and coastal waters. In storm conditions, open oceans tend to have more swell dominated spectra than wind dominated spectra and the opposite is true for fetch limited coastal waters.
Following Guedes-Soares, the double-peaked spectra were represented by the sum of a low and a high frequency JONSWAP spectrum. Spectra used in the simulations for both swell dominated open ocean and fetch limited coastal waters are given in figures 3 and 4. Significant wave heights were chosen as 7 m and 9 m and periods 7.5 sec and 11 sec for wind and swell waves respectively.

5. MOTION RESPONSE SIMULATION OF SEMI-SUBMERSIBLES IN OPEN OCEAN AND COASTAL WATERS IN EXTREME WEATHER CONDITIONS

Results of the simulations are plotted in figures 5 to 15. The FFT analyses of each time series are also plotted in the same graph. In order to carry out the FFT analysis a NAG library routine was utilised, which gives twice the real value of zero frequency (steady) components. The current speed was chosen as 1.5 m/sec and wind 33 m/sec. The simulation time was chosen to be 32768s. In order to avoid shock responses, an exponential ramp function was applied to the external forces for the first 3000 seconds. Wind gustiness was created using the Ochi-Shin wind spectrum [Ochi and Shin 1988]. Drift forces in all simulations were calculated using a 3-D program developed by Chan [1990]. Slowly varying wave forces were calculated using the JONSWAP wave spectrum and the mean drift forces in regular waves [Newman 1974; Pinkster 1974]. Swell waves were treated in the same way as wind waves: both have first and second order effects on the semi-submersible

and the calculation procedures for these forces are the same. A typical storm profile given by Morton [1995] indicates that at the storm peak all forces tend to become collinear with the exception of swell waves which have an average of 15 degrees directional difference from the others. Because of that, simulations were repeated for different swell directions, 0 to 40 degrees for open ocean and 0 to 20 degrees for coastal waters. In all simulations thrusters were used effectively. Details about the thruster model are given in Yilmaz and Incecik [1995].

(a) Simulations in swell dominated open ocean

Significant wave heights of 7 and 9 m and wave periods of 7.5 and 11 sec for wind and swell waves respectively were chosen to simulate the double-peaked wave spectrum for the open ocean (figure 3). Effect of swell and wind waves on the wave frequency motions are presented in figures 5 to 7 where the source of excitation are first order wind and swell waves. Swell and wind wave's spectrum peaks are 0.44 and 0.63 rad/sec respectively. Figure 5 shows the combined first order effect of co-linear wind and swell waves, which is dominated by swell waves; 2.31 m at 0.44 rad/sec and 0.72 m at 0.63 rad/sec for surge motions. The same observations can be made for the heave responses and mooring forces. In figures 6 and 7, swell wave heading is varied to 20 and 40 degrees. As expected, with the change in the swell direction from 0 to 40 deg. sway and yaw amplitudes increase. The same trend can also be observed for mooring forces in the sway direction and for mooring moments. For all motions, responses at the swell wave spectrum peak are higher than those at the wind wave spectrum peak. It can be concluded from these results that while the swell waves dominate the first order responses, the wind waves' contribution to the steady responses are bigger than those of swell despite the swell dominance in the spectrum. Irregular seas also excite the natural frequencies of the system, which are 0.036 for surge, 0.0307 rad/sec for sway and 0.255 for heave. Yaw response is almost completely dominated by the oscillations in yaw natural frequency, which is 0.0268 rad/sec. In figures 5 to 7, apart from the wave frequencies, there are responses in sub and super harmonics. Some of these harmonics correspond to the natural frequencies and others occur at fractions and multiples of the wave frequencies. This behaviour with sub and super harmonics is a characteristic of non-linear systems, which are distinct from the response of linear systems.

Figures 8 and 9 show the motion responses and mooring forces due to the slowly varying excitation for the swell directions corresponding to figures 6 and 7. Due to the high current and wind speed, wind and current have the biggest steady effects on the surge motion. It can be observed from these figures that surge and sway responses are not greatly affected by the change in swell direction. One possible reason for this is the presence of a strong current and wind acting collinearly in the surge direction, causing a high mean tension on the mooring lines. As expected the yaw response increases with the change in sway direction from 0 to 40 degrees. In the absence of high frequency excitation, responses in figures 8 and 9 are completely determined by low frequency oscillations which correspond to the natural frequencies of the system.

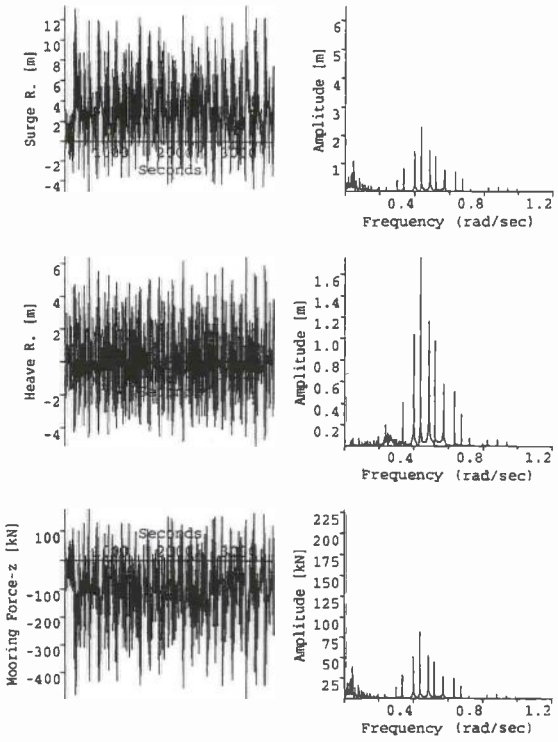

Figure 5. Motion responses and mooring forces. First order wave excitation in open ocean. Collinear wind and swell waves.

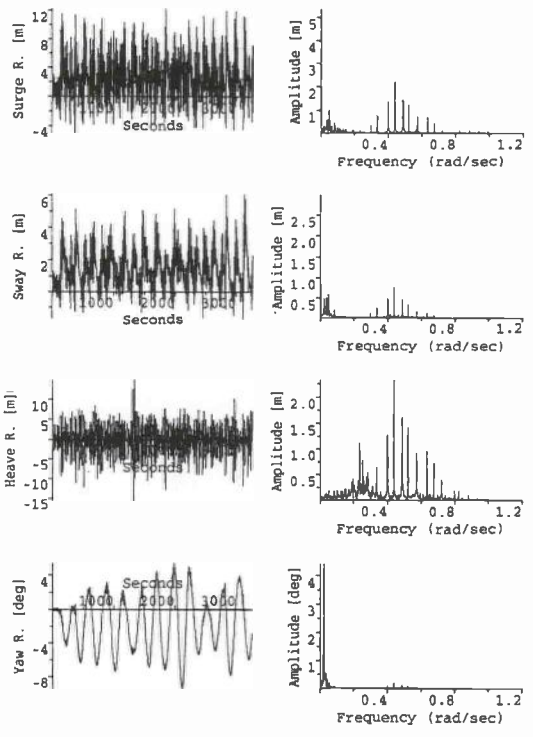

Figure. 6a. Motion responses. First order wave excitation in open ocean. Wind wave heading = 90 degrees, swell wave heading = 70 degrees.

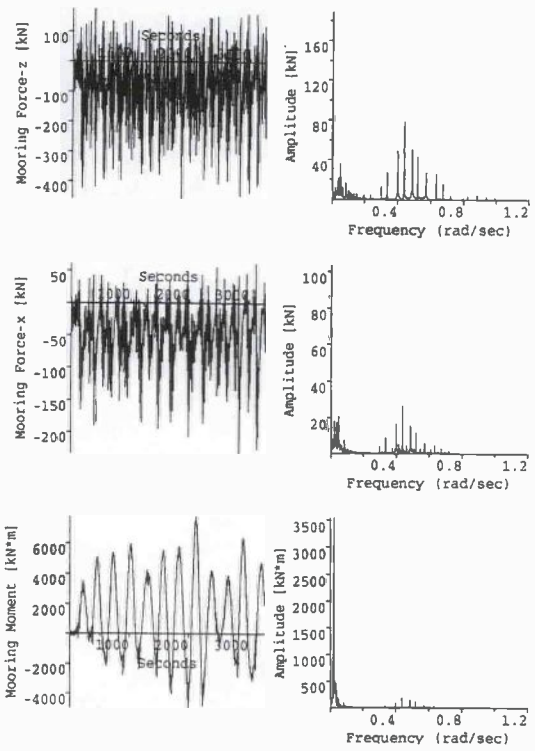

Figure 6(b). Mooring forces and moment corresponding to figure 6(a).

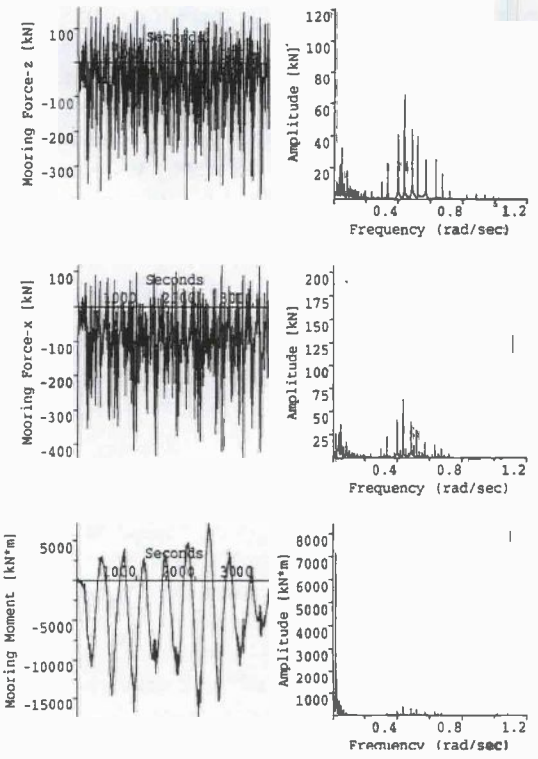

Figure 7(b). Mooring forces and moment corresponding to figure 7(a).

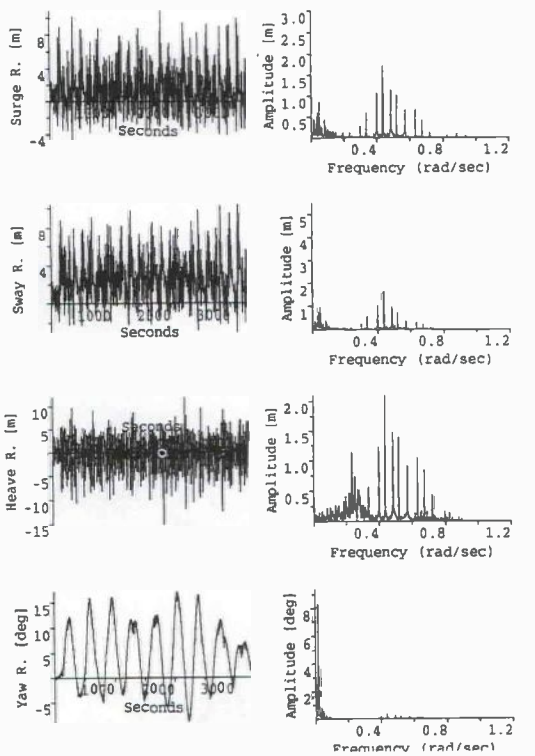

Figure 7a. Motion responses. First order wave excitation in open ocean. Wind wave heading = 90 degrees, swell wave heading = 50degrees.

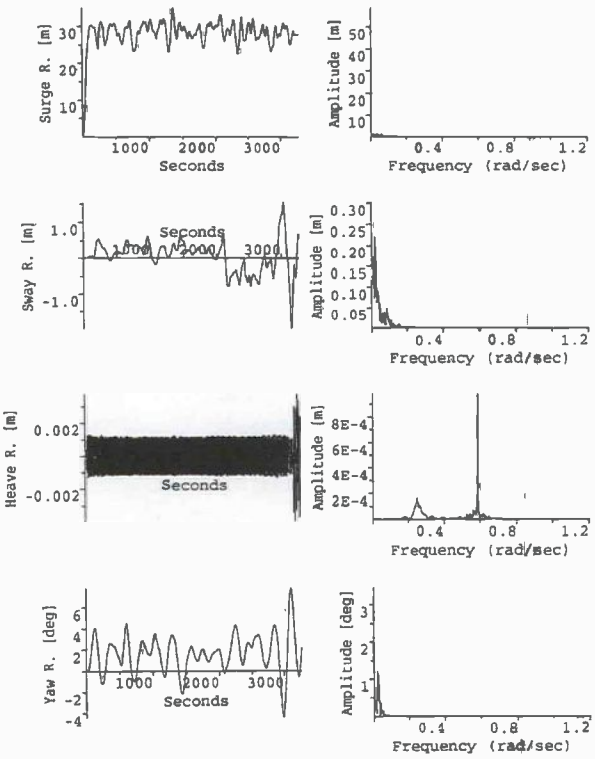

Figure 8a. Motion responses. Slowly varying and steady excitation in open ocean. Swell wave heading = 70 degrees, wind and current directions = 90 degrees.

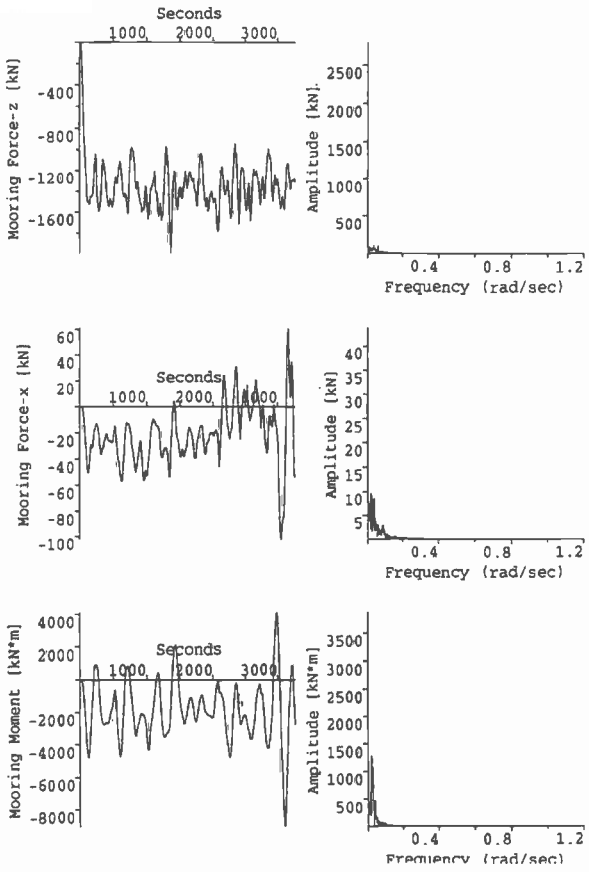

Figure 8(b). Mooring forces and moment corresponding to figure 8(a).

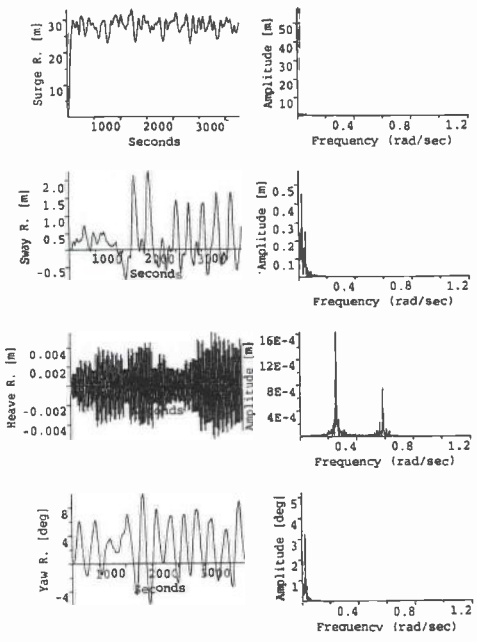

Figure 9(a). Motion responses. Slowly varying and steady excitation in open ocean. Swell wave heading = 50 degrees, wind and current directions = 90 degrees.

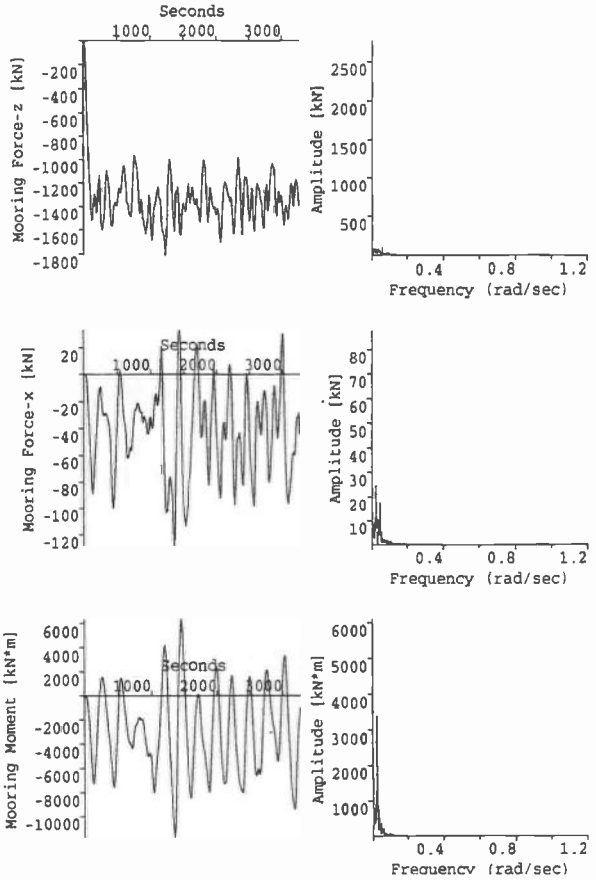

Figure 9(b). Mooring forces and moment corresponding to figure 9(a).

(b) Simulations in wind dominated coastal waters

Significant 9m and 7m wave heights and wave periods of 7.5 seconds and 13 seconds for wind and swell waves respectively were chosen to simulate the double-peaked wave spectrum for coastal waters (figure 4). The swell and wind wave's spectrum peaks are 0.44 and 0.63 rad/sec respectively. During the simulations swell direction was varied from 0 to 20 degrees. It was thought that swell direction would vary less in coastal waters due to the presence of land that obstructs the wave propagation from some sectors and because swells in coastal waters have a higher probability of being wind dominated. Figures 10 to 12 show the responses and mooring forces caused by the first order wave forces and figures 13 to 15 show the responses and mooring forces caused by slowly varying forces. Despite the wind dominance in the wave spectrum (figure 4), the first order motion responses (figures 10 to 12) of 0.4 rad/sec at the swell wave spectrum peak were still higher than 0.63 rad/sec. at the wind wave spectrum peak. The same observations were made for a swell dominated open ocean where the changes in the swell direction caused an increase in the sway and yaw responses. One observed difference between the first order responses in swell and wind dominated seas was that maximum responses in swell dominated seas were higher than those in wind dominated seas.

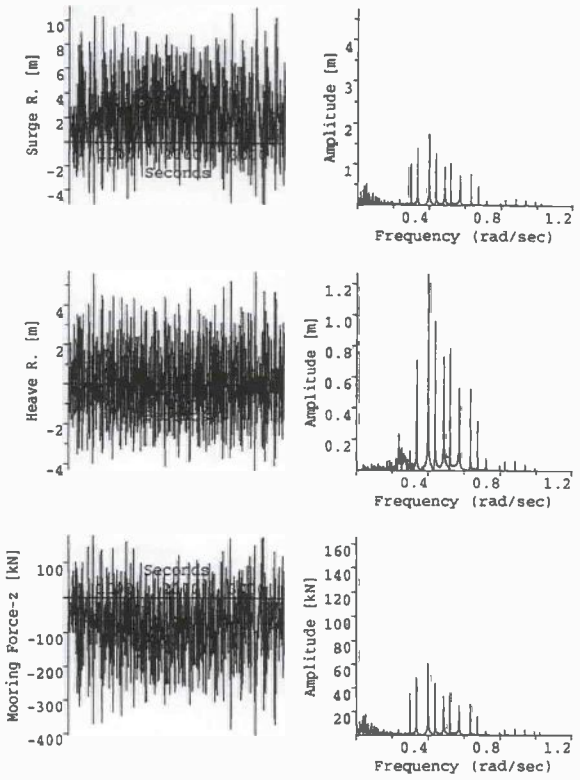

Figure 10. Motion responses and mooring forces. First order wave excitation in coastal waters. Collinear wind and swell waves.

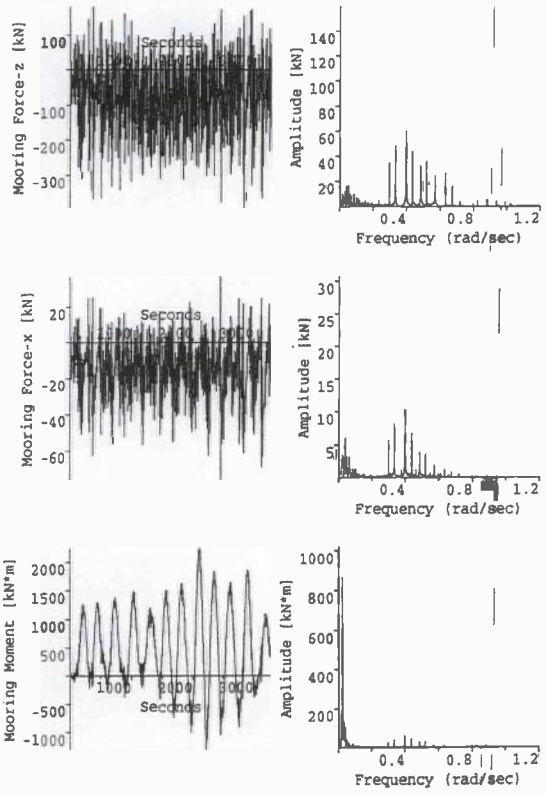

Figure 11(b). Mooring forces and moment corresponding to figure 11(a).

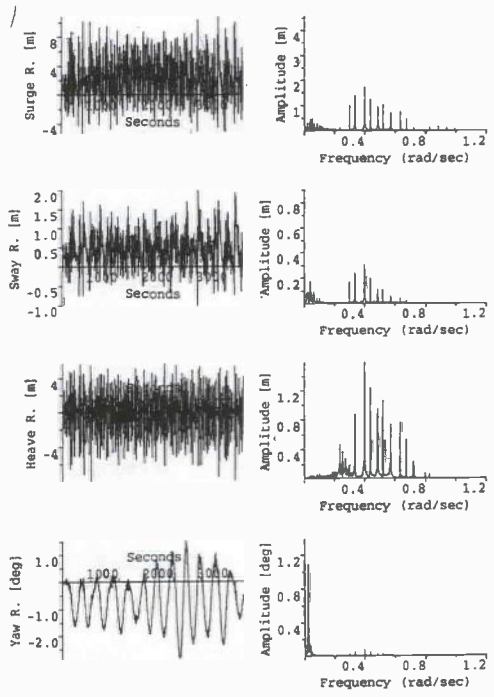

Figure 11(a). Motion responses. First order wave excitation in coastal waters. Wind wave heading = 90 degrees, swell wave heading = 80 degrees.

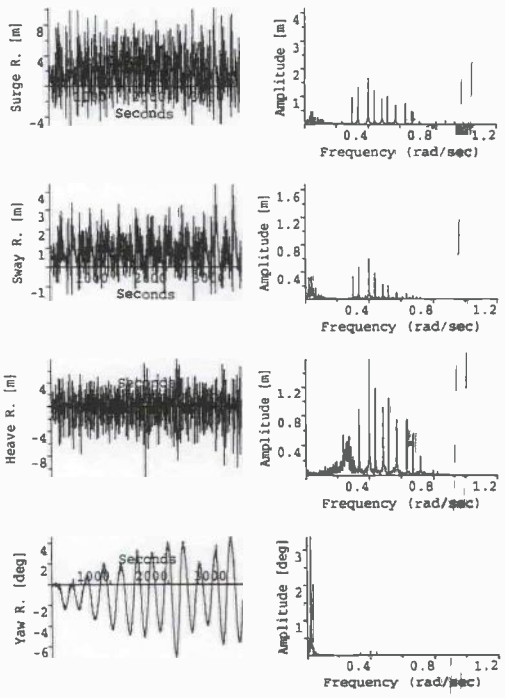

Figure 12(a). Motion responses. First order wave excitation in coastal waters. Wind wave heading = 90 degrees, swell wave heading = 70 degrees.

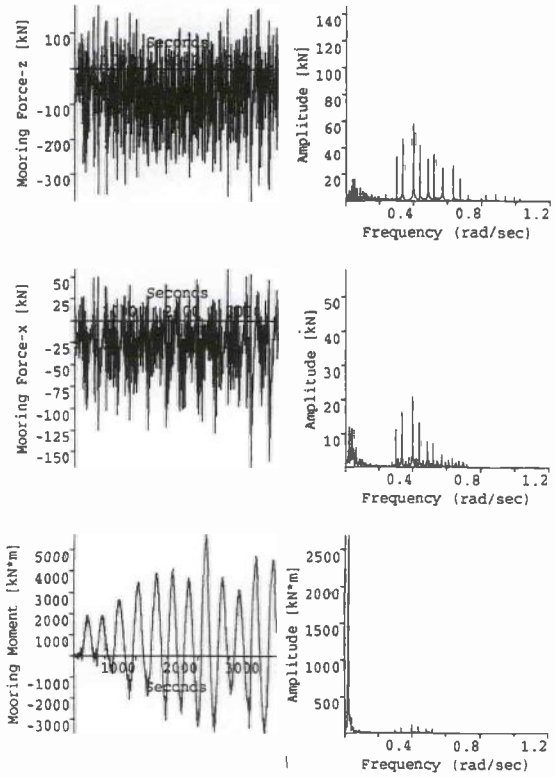

Figure 12(b). Mooring forces and moment corresponding to figure 12(a).

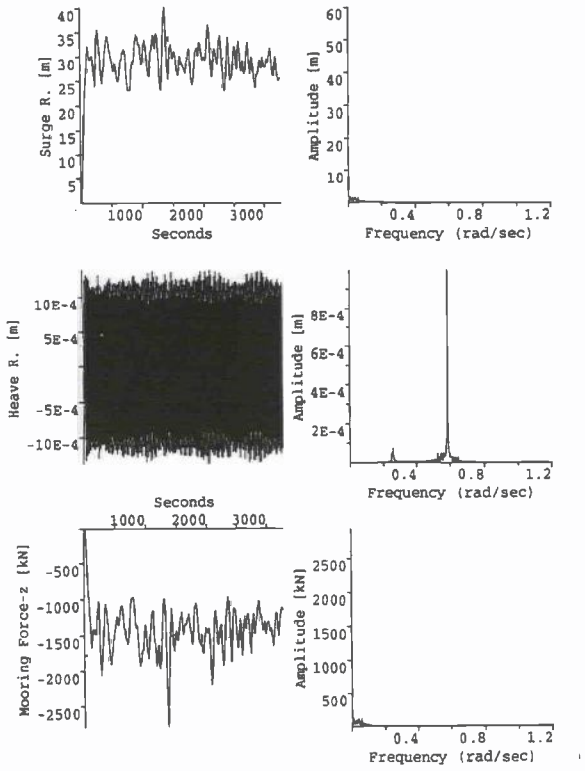

Figure 13. Motion responses and mooring force. Slowly varying and steady collinear excitation in coastal waters.

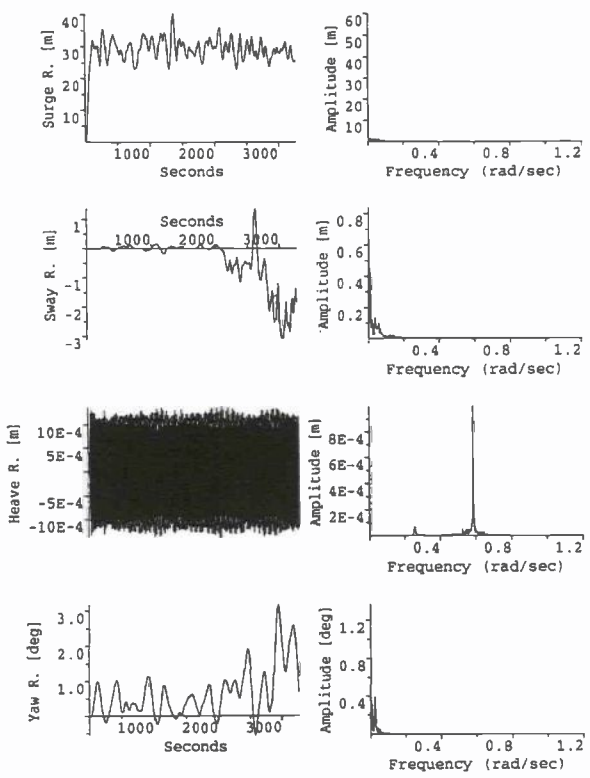

Figure 14(a). Motion responses. Slowly varying and steady excitation in coastal waters. Swell wave heading = 80 degrees, wind and current directions = 90 degrees.

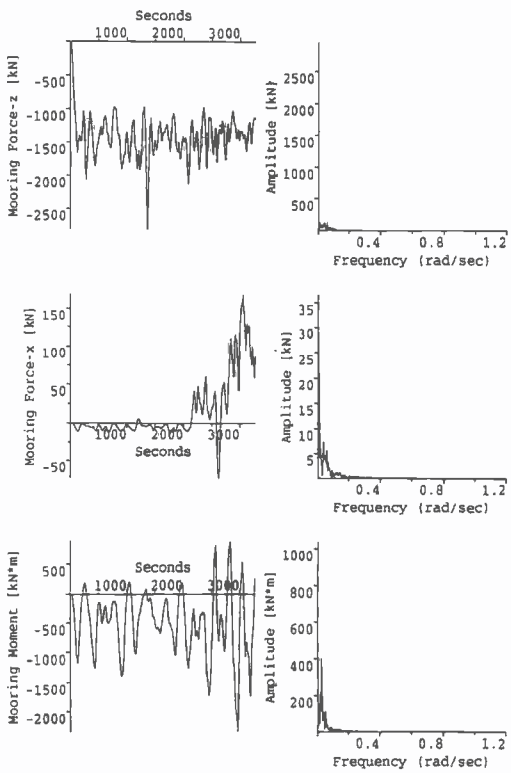

Figure 14(b). Mooring forces and moment corresponding to figure 14(a).

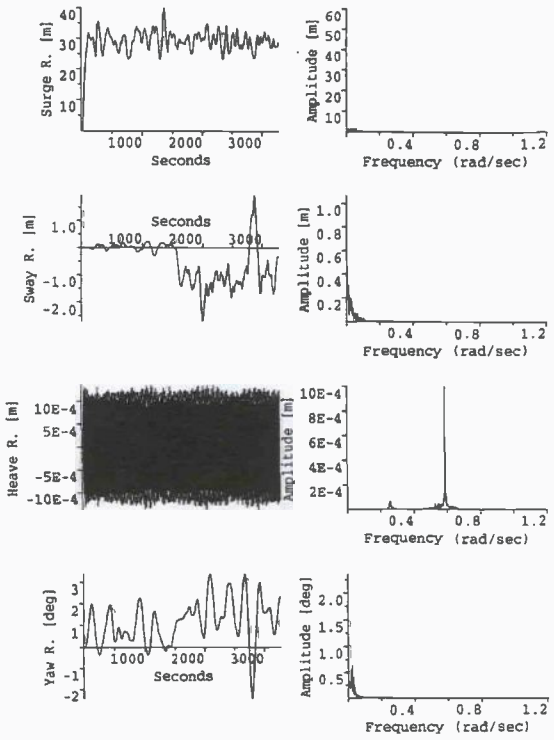

Figure 15(a). Motion responses. Slowly varying and steady excitation in coastal waters. Swell wave heading = 70 degrees, wind and current directions = 90 degrees.

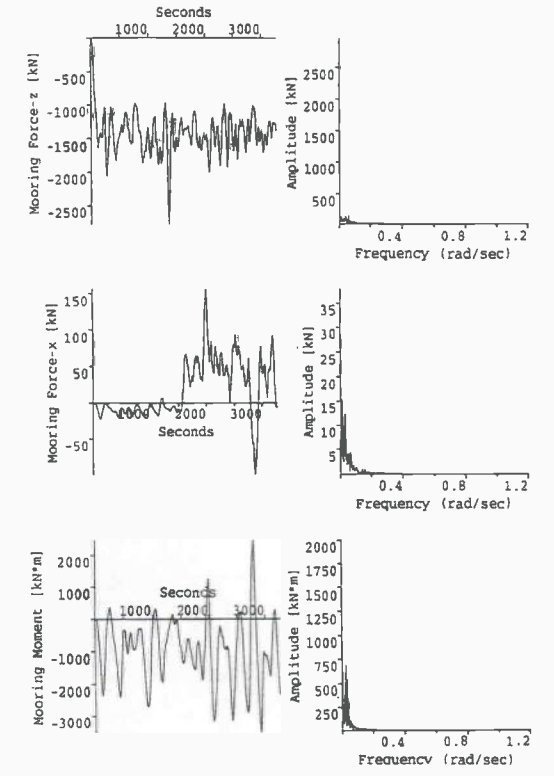

Figure 15(b). Mooring forces and moment corresponding to figure 15(a).

With a change in swell direction from 0 to 20 degrees the sway and yaw responses due to slowly varying forces increased and showed some chaotic behaviour with sudden jumps (figures 13 to 15). This could be due to the very high mean tension on the mooring lines exerted by current and wind. Maximum values of steady responses in wind dominated seas were much higher than those in swell dominated seas. This is expected because steady forces are the result of high frequency wind waves which dominate the low frequency swell waves in wind dominated seas.

6. OVERALL CONCLUSIONS

1. Wind and current have the largest steady effects on the surge motion.
2. Maximum first order responses in swell dominated seas are higher than those in wind dominated seas.
3. Steady responses in wind dominated seas are much higher than those in swell dominated seas. This is due to the steady forces that resulted from high frequency wind waves which dominate the low frequency swell waves.

REFERENCES

American Bureau of Shipping. 1973 *Rules for building and classing mobile offshore drilling units.*

Chan, H.S. 1990 A three dimensional technique for predicting first and second order hydrodynamic forces on a marine vehicle advancing in waves. *Doctoral Thesis.* University of Glasgow, Department of Naval Architecture and Ocean Engineering.

Incecik, A. 1982 Design aspects of the hydrodynamic and structural loading on floating offshore platforms under wave excitation. *Doctoral Thesis.* University of Glasgow, Department of Naval Architecture and Ocean Engineering.

Guedes-Soares, C. 1984 Representation of double peaked sea wave spectra. *Ocean Engineering.* **11** (2) 185-207.

Morton, I.D. 1995 A portfolio of wind and wave data for several storm events in the north sea and the north Atlantic. *Maderia Project Report No. 6.* University of Stirling, Department of Management and Organization.

The NAG Fortran Library Manual-Mark 14 1992 **7** Numerical Algorithms Group Ltd.

Newman, J.N. 1974 Second order slowly varying forces on vessels in irregular waves. *Proceedings of the International Symposium on Dynamic Marine Vehicles Structures in Waves.* 182-186. London.

Ochi, M.K. & Shin, Y.S. 1988 Wind turbulent spectra for design consideration of offshore structures. *Proceedings of Offshore Technology Conference.* Paper No. **5736.** 461-467. Houston.

Pinkster, J.A. 1974 Low frequency phenomena associated with vessels moored at sea. *Society of Petroleum Engineers. American Institute of Mining.* Paper No. **SPE3837.**

Pinkster, J. A., Incecik, A., Collins, J. I., Fylling, I. J., Ikegami, K., Maeda, H., Romeling, J., U., Sevastiani, L., Vassilev, P. 1993 The Ocean Engineering Committee, Final Report and Recommendations, 20th International Towing Tank Conference, San Francisco.

Söylemez, M. 1996 A general method for calculating hydrodynamic forces. *Ocean Engineering*. **23** (5) 423-445.

Söylemez, M. 1990 Motion response simulation of damaged floating platforms. *Doctoral. Thesis*. University of Glasgow, Department of Naval Architecture and Ocean Engineering.

Yilmaz, O. & Incecik, A. 1995 Dynamic response of moored semi-submersible platforms to non-collinear wave, wind, and current loading. *Proceedings of 5th International Offshore and Polar Engineering Conference (ISOPE)*. The Hague.